14

LAL-RT-97-05

FERMILAB
NOV 2 1998
LIBRARY

Fermilab Library
0 1160 0067901 3

LAL/RT 97-05
December 1997

Laboratoire de l'Accélérateur Linéaire

A low noise transceiver for the NA48 liquid kryton calorimeter

C. de la Taille, G. Martin-Chassard and N. Seguin-Moreau

Laboratoire de l'Accélérateur Linéaire
IN2P3-CNRS et Université de Paris-Sud, BP 34, F-91898 Orsay Cedex

U.E.R
de
l'Université Paris-Sud

Institut National
de Physique Nucléaire
et de Physique des Particules

B.P. 34 ~ Bâtiment 200 ~ 91898 ORSAY CEDEX

LAL/RT 97-05
December 1997

A LOW NOISE TRANSCEIVER FOR THE NA48 LIQUID KRYPTON CALORIMETER

C. de la Taille, G. Martin-Chassard and N. Seguin-Moreau

Laboratoire de l'Accélérateur Linéaire, IN2P3-CNRS et Université Paris-Sud
BP 34 - 91898 Orsay Cedex, France

Abstract

The NA48 transceiver consists of a pole-zero compensation from 150 ns down to 10 ns and a differential line driver which delivers up to ± 1.5 V into 50 Ω. A circuit, using surface mounted components, has been realized and has equipped the 15,000 channels of the liquid Krypton calorimeter since summer 1996 ; it is described along with its performances.

1 Introduction

The NA48 liquid krypton calorimeter is designed to achieve high precision measurements for kaons decaying into π^0s (neutral channel), for which the noise performance of the front end electronics is an important issue [1]. Therefore, low noise charge preamplifiers, optimized for operation at low temperature, are mounted directly on the electrodes to amplify the ionization current from the detector. However, its long feedback time constant is incompatible with the early gain selection in the Calorimeter Pipelined Digitizer (CPD) used in the readout to fit the 14 bits dynamic range in the 10 bit FADCs. Moreover, the large number of towers (121) summed to reconstruct a shower requires a very low coherent noise, which advocates for a differential connection between the cryostat and the readout in the barracks. These functions are performed by circuits located right on the feedthroughs and referred to as transceivers.

In the first part, we will analyse the various elements of the front end electronics, with an emphasis on the preamplifiers as they set the noise requirements for the transceivers. In the second part, we will describe the architecture of the transceiver circuit. Then, we will present the measurement results of the final version, which has equipped the 15,000 channels of the calorimeter since summer 1996.

2 Front End electronics

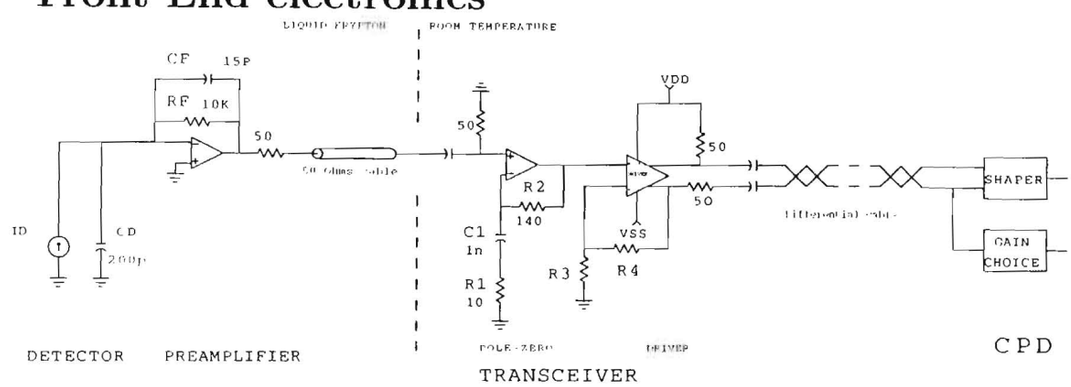

Figure 1: Schematic diagram of the front end electronics

2.1 Detector and Signal

The detector has already been largely described [2]. It is an almost homogeneous liquid krypton calorimeter, aimed at high precision energy measurements of photons below 100 GeV. It is segmented in around 15,000 towers 2×2 cm^2 area and 1.25 m long, to achieve 27 X_0 depth and minimize longitudinal leakage.

The motion of the ionization electrons with the electric field applied (E = 10 kVcm^{-1}) induces a triangular current, whose initial value is typically $I_0 = 2.5$ μA/GeV and which decays in the drift time $t_{dr} = 3$ μs. Ideally, the decay is linear if the charge

is uniformly distributed across the gap, but here the shower develops almost parallel to the electrods, with only a small accordion shape to smooth the ionization across the gap. Therefore, the signal shape depends on the shower profile, and to get a good timing information indepedently of the impinging position, a fast shaping is used ($t_p(\Delta) = 40$ ns) to be sensitive only to the initial current.

The electronic modelization of the detector is traditionally done by a current source in parallel with a capacitance to ground $C_d \approx 200$ pF (cf. fig.1), although here the length of the detector makes it more similar to a transmission line of 70 Ω impedance and 6 ns delay. The large gap, which gives a small detector capacitance to ground and a good noise performance, has a counterpart in a relatively large crosstalk between adjacent cells, with a coupling capacitance of the same order than the capacitance to ground.

2.2 Preamplifier

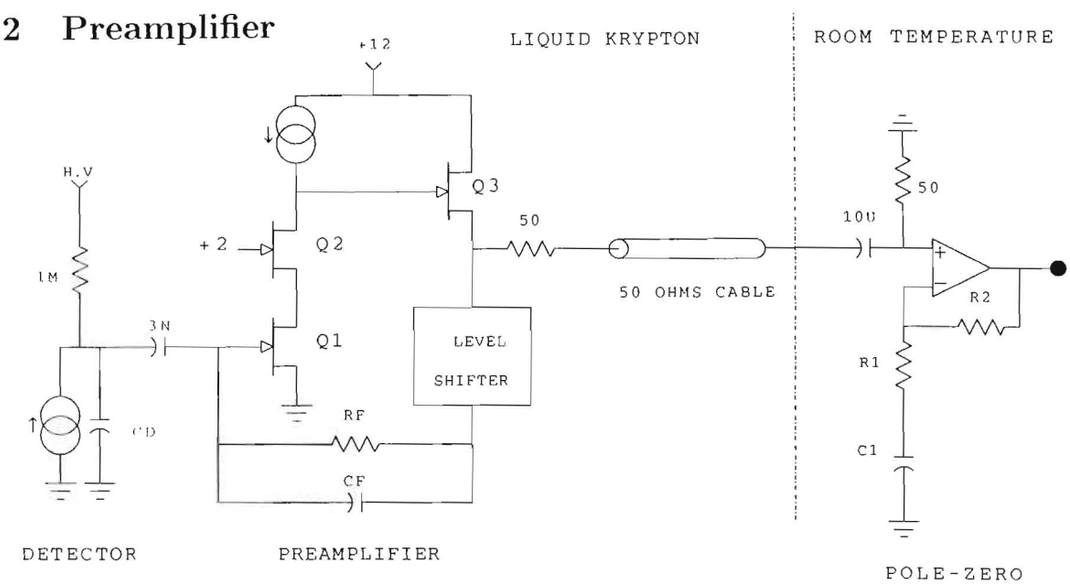

Figure 2: Schematic diagram of the preamplifier followed by the pole-zero compensation of the transceiver

Each detector tower is read out by a preamplifier, located directly at the back of the calorimeter inside the LKr in order to minimize the electronics noise[1]. The preamplifer follows the classical transimpedance architecture, as shown in fig.2, with a common source FET (Q1) followed by a cascode (Q2) and a source follower (Q3) [4]. The transistors are silicon junction FETs, optimized for low temperature operation[2]. As a matter of fact, the optimum noise performance[3] is achieved at around 120 °K, which nicely corresponds to liquid krypton.

[1] The use of warm preamps (ØT) [3] would deteriorate the noise performance as the detector capacitance is relatively small and the shaping not very fast.

[2] These transistors are manufactured by Interfet Corporation. Their doping levels are set to minimize carrier freezout which otherwise leads to the collapse of the transconductance g_m at low temperature.

[3] It has been widely observed that below 200 °K, the thermal noise of the FET does not follow the usual equation : $e_n^2 = 4kT\alpha/g_m(T)$ where g_m is the transconductance of the FET (and varies with temperature)

The transfer function of the preamplifier, shown in fig. 3(a), is given by[4] :

$$H_{pa}(s) = \frac{V_{out}(s)}{I_{in}(s)} = \frac{-R_f}{1 + s\tau_f} \tag{2}$$

with the notations of fig.2, $\tau_f = R_f C_f$ and $s = j\omega$ the complex frequency. In 1995 H4 test beam, two values have been used $\tau_f = 500$ ns ($R_f = 33$ kΩ, $C_f = 15$ pF) and $\tau_f = 150$ ns ($R_f = 10$ kΩ, $C_f = 15$ pF). The higher value of R_f gives a larger output amplitude after a longer time, but has absolutely no influence on the amplitude after shaping[5]. This charge sensitive configuration[6] exhibits a low real input impedance[7] R_{in}, often referred to as an "electronically cooled" resistor [5], $R_{in} = (1/g_m)(C_0/C_f)$ in which g_m is the transconductance of the input transistor and C_0 is the dominant pole capacitance (on the drain of Q2). It can be set to terminate the detector "transmission line" in its characteristic impedance [6] and thereby minimize reflections which can deteriorate the energy resolution and crosstalk. This requires a minimal value for C_f around 10 pF[8]. This rather large value for a detector of 200 pF leads to a small "noise gain" given by[9] C_d/C_f. At the shaper central frequency, the dominant noise is the series term e_n given by Q1 ($e_n \approx 0.58$ nV/$\sqrt{\text{Hz}}$ at 120 °K). As shown in fig. 3(b), the noise at the preamp output, obtained by multiplying e_n by the "noise gain", is 7.7 nV/$\sqrt{\text{Hz}}$, further decreased by a 6 dB loss due to the cable termination at both ends[10]. Thus, the second stage noise becomes an important consideration.

The signal at the preamplifier output is obtained by convoluting the detector triangular current with the preamp transfer function. It looks like a rising exponential with a

---

and $\alpha \approx 0.67$. The noise even soars below 100 °K, to higher levels than at room temperature, which is often attributed to hot electrons and non equilibrium with the lattice.

[4]A more accurate formula would be :

$$H_{pa}(s) = \frac{-R_f}{R_f C_d s^2/\omega_c + R_f C_f s + 1} \tag{1}$$

in which ω_c is the unity gain frequency of the preamplifier. The stability of this second order system requires the 2 poles to be sufficiently separated ; the quality factor being : Q = $(1/C_f)\sqrt{C_d/\omega_c R_f}$, $Q < 0.5$ ensures stability.

[5]With a shaper performing a differentiation and several integrations giving a shaping time of 40 ns (cf. 2.4), what matters is only the signal slope, which is determined by C_f. This can also be seen in fig. 3 (a), where the gain at the central frequency of the filter ($\approx$ 4 MHz) is right on the slope $1/j\omega C_f$. R_f determines only the low frequency gain, which is anyway strongly attenuated by the shaper.

[6]The transimpedance configuration is called "charge sensitive" when $\tau_f > t_p$ where t_p is the shaping time and "current sensitive" otherwise. This simply refers to the fact that the transimpedance is constant (R_f) or decreasing with frequency ($1/j\omega C_f$) at the central frequency of the shaper

[7]Conversely, the current sensitive configuration exhibits an inductive input impedance : L = R_f/ω_c

[8]With a large NJ450 Si JFET transistors from Interfet, $g_m \approx 25$ mA/V at $I_D = 4$ mA and T = 120 °K. $C_0 \approx 25$ pF, which leads to $C_f = 15$ pF to achieve 70 Ω input impedance. It can be easily measured by plotting the rise time to the impulse response as a function of the detector capacitance.

[9]The precise formula would be : $(C_d + C_0 + C_f)/C_f$

[10]There have been many attempts to remove this loss, by terminating the cable on one side only :

- removing the resistor in series at the sending end makes a too heavy load for the preamp, exceeding the I_{DSS} of Q3.
- raising the resistor to ground at the receiving end makes a -100 % reflection which cannot be absorbed by the preamplifier without perturbating the feedback and creating oscillations.

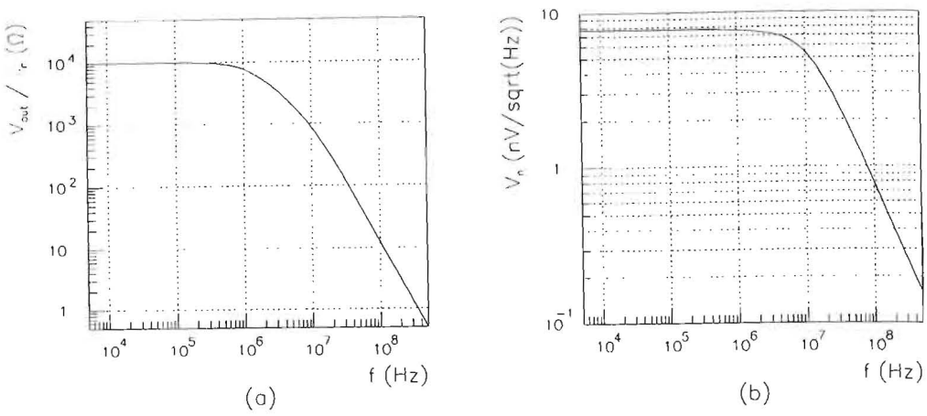

Figure 3: Transfer function (a) and output noise (b) of the preamplifier shown in fig. 2 as a function of frequency, with $R_f = 10$ kΩ, $C_f = 15$ pF and $C_d = 200$ pF.

time constant τ_f decaying in the typical drift time (3 μs) (cf. fig. 4(b) : input signal of the transceiver).

2.3 Transceiver

The transceivers are located directly on the feedthroughs and share the Faraday cage formed by the cryostat. They terminate the coaxial cables from the preamplifiers into 50 Ω. A pole-zero compensation stage (cf. fig.1) turns the preamp time constant τ_f into a faster value τ_1 of 10 ns, in order to enable a fast gain selection in the readout (cf. 2.4). The transfer function of this circuit is :

$$H_{pz}(s) = \frac{1 + s(R_1 + R_2)C_1}{1 + sR_1C_1} \tag{3}$$

By letting $(R_1 + R_2)C_1 = R_fC_f$, the signal has a faster pole $\tau_1 = R_1C_1$. The price paid for accelerating the signal is a loss of amplitude of typically τ_f/τ_1, which is compensated for by a similar amplification in the pole-zero amplifier. This is shown in fig.4(a) which plots the transfer function as a function of frequency. Thus, going from 150 ns to 10 ns requires a gain of 15.

Both, the long distance between the cryostat and the readout (10 meters) and the need of precision which requires a very low coherent noise, advocates for a differential transmission. The output stage is a differential line driver to transmit the signals on a shielded twisted pair in order to minimize crosstalk and electromagnetic interferences. It includes an extra amplification to match the input voltage requirement from the readout, and compensate for the 6 dB attenuation due to the cable termination at both ends.

The transfer function of the preamplifier plus the transceiver becomes :

$$H_{pa+tx}(s) = \frac{V_{outtx}(s)}{I_{inpa}(s)} = \frac{-R_f}{1 + s\tau_1}\frac{R_3 + R_4}{R_3} \tag{4}$$

The signal at the transceiver output is obtained by convoluting the detector triangular current with this transfer function. It looks like a rising exponential with a time constant $\tau_1 = R_1C_1$ decaying in the typical drift time (3 μs) as shown in fig. 4(b).

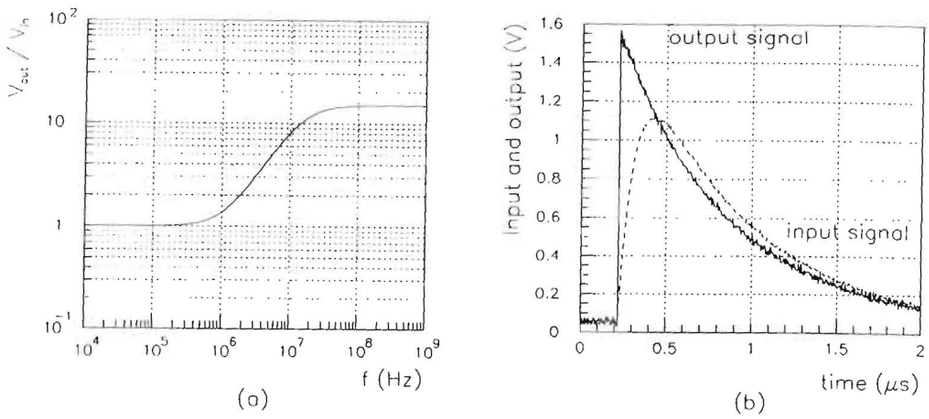

Figure 4: Transfer function of the transceiver as a function of frequency (a) and input and output signals as a function of time (b).

Two circuits have been studied for this purpose : an ASIC [7] and a discrete version. The integrated circuit arrived too late to be chosen. Therefore, only the discrete transceiver, mass produced, is presented in this paper.

2.4 Calorimeter Pipelined Digitizer (CPD)

The signal readout consists of a differential receiver for analog signals, with 14 bits dynamic range, followed by a fast shaper. During the shaping, a gain selection system on the input signal induces a gain switching, after the shaper, at the input of a 10 bit Flash ADC. Then, this converted signal is stored in a digital pipeline. This system is known as CPD [8]. A simplified schematic of the input stage and filter of the CPD is shown in fig. 5. The CPD boards are located in the electronics racks, 10 meters away from the detector.

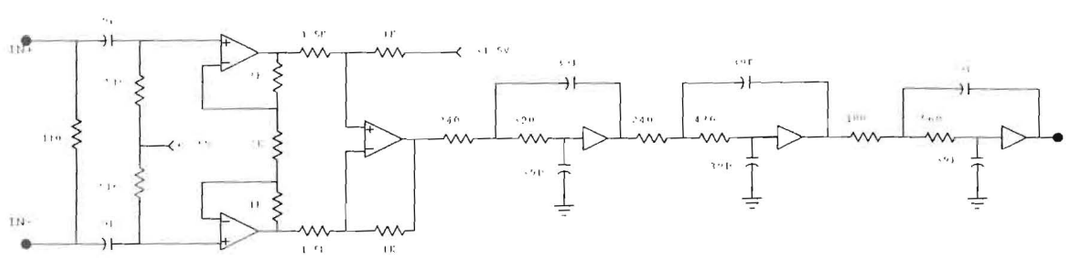

Figure 5: Schematic diagram of the input stage and filter of the CPD

3 Transceiver design

3.1 Requirements

From sections 2.1, 2.2, 2.3 and 2.4, the requirements for the transceiver can be summarized as follows :

•**Input impedance : 50 Ω**, to terminate properly the coaxial cables coming from the preamplifiers inside the cryostat.

•**Input noise : < 2 nV/√Hz**, in order not to deteriorate the noise performance of the preamplifers, given the small noise gain in the preamps (cf. fig. 3(b)).

•**Output rise time: < 25 ns (10-90%)** to allow proper gain selection in the CPD. It corresponds to a rise time constant around 10 ns.

•**Transceiver gain : ± 1 V** at the output of the transceiver after the twisted pair for a 125 μA (50 GeV) signal at the preamplifier input in order to match the dynamic range in the CPD.

•**Linearity : < 0.1 %** to be able to measure accurately a signal on top of an accidental.

•**Area : 110 × 220 mm^2 for 32 channels** to fit right on the feedthroughs.

•**Power dissipation and cost : as low as possible** because of the large number of channels (15,000).

3.2 Architecture

The schematic of one channel of the transceiver is shown in fig. 6. The first stage of

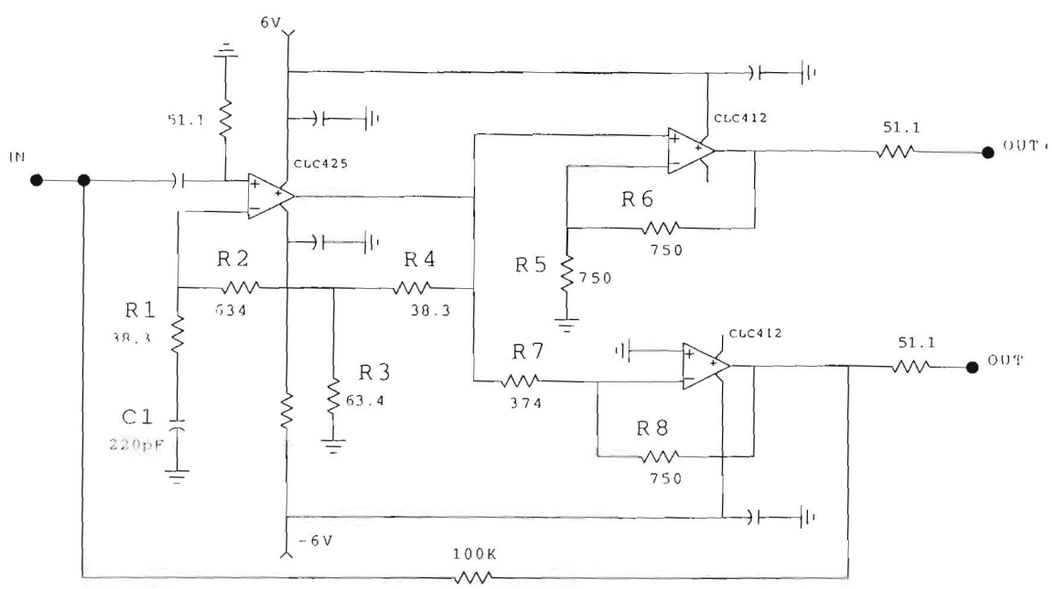

Figure 6: Schematic diagram of one channel of the transceiver

the transceiver is built around a low noise operational amplifier[11](opamp). The large bandwidth product of this opamp allows to perform in the same stage the pole-zero cancellation and the additional gain without sacrificing speed and linearity.

The transfer function of this first stage is given by :

$$H_{tx}(s) = \frac{V_{out}(s)}{V_{in}(s)} = \frac{R_3 + R_4}{R_3} \frac{1 + s(R_1 + R_2 + R_3 \parallel R_4)C_1}{1 + s\tau_1} \tag{5}$$

The time constant $\tau_1 = R_1 C_1$ is chosen to be less than 10 ns to have the right rise time for the output signal. R_1 must not be too small ($> 20\ \Omega$), in order to avoid oscillations due to parasitic inductance, but not too high for low noise ; taking $R_1 = 38.3\ \Omega$, the value of the capacitance becomes : $C_1 = 220$ pF. R_3 and R_4 are chosen to set the extra gain given by $(R_3 + R_4)/\ R_3$. A gain of 1.6 is expected so the resistors are set to : $R_3 = 63.4\ \Omega$ and $R_4 = 38.3\ \Omega$. The value of R_2 is measured to perform the pole-zero cancellation with preamplifiers working at liquid krypton temperature, such that :

$$(R_1 + R_2 + R_3 \parallel R_4)C_1 = \tau_f \tag{6}$$

giving $R_2 = 634\ \Omega$.

A differential driver can be done by using the voltage and current outputs of the output transistor (cf fig.1). This method gives an excellent symmetry on the output signals provided the impedances on emitter and collector are equal. Unfortunately, the rejection of noise pick up on the cable is poor as any current on the direct output is mirrored on the inverting output. With discrete components, it is thus preferable to use a classical differential driver obtained with two buffers built around a dual opamp[12]. The output signals are series terminated by 51.1 Ω resistors ; the gain of the buffers is two[13] to compensate the loss of signal due to the termination of the cable at both ends.

A large resistor (100 KΩ) has been inserted between the direct input and the inverted output to know the output DC voltage of the preamplifier (when the power supplies of the transceivers are off) in order to be able to localize the breakdown in case of bad channel.

3.3 Summation circuit

At the beginning of the experiment, it was necessary to provide the sum of various channels accurately chosen. The transceiver board was also designed to do these summations. 16 signals coming from the preamplifiers are summed together and then, 32 sums go through a dedicated transceiver board, which perform the pole-zero cancellation, to the CPD system. To provide a fast signal to the CPD, the summation circuit must not add a new dominant pole to the transfer function of the transceiver.

The schematic of the summation circuit is shown in fig. 7. It consists of a fast pnp transistor, used in common base configuration to sum the 16 channels, followed by

[11]The opamp used is a CLC425 distributed by Comlinear Corporation which exhibits very good performances such as an input noise of 1 nV/$\sqrt{\text{Hz}}$ and a gain bandwidth product of 1.7 GHz.

[12]This dual opamp is a CLC412 distributed also by Comlinear Corporation and has a bandwith of 250 MHz.

[13]The gain of these buffers is given by $(R_5 + R_6)/R_5$ for the positive output and by $-R_8/R_7$ for the inverted output.

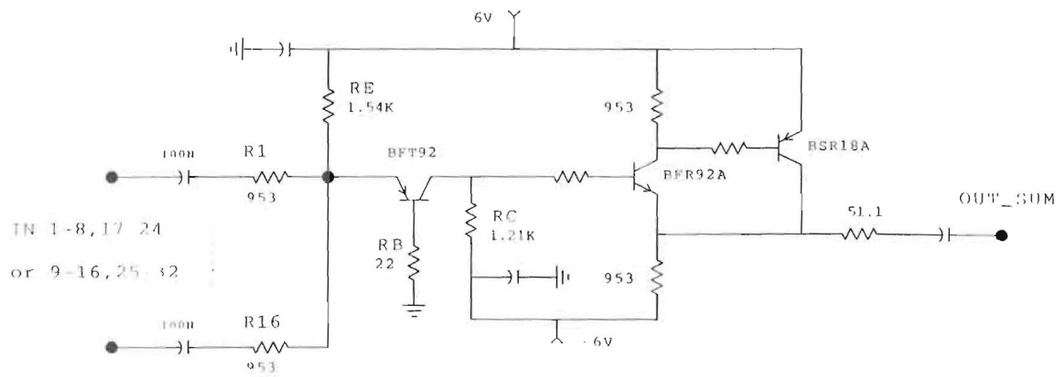

Figure 7: Schematic diagram of the summation circuit

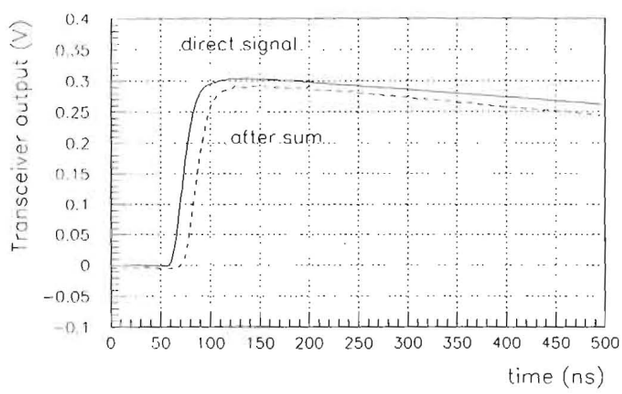

Figure 8: Output signal of the transceiver after the summation circuit compared to the direct output

a White follower output stage which drives a 2 meter long coaxial cable to the dedicated transceiver board. As the maximum energy in the 16 summed channels is 65 GeV, to fit the dynamic range of the preamplifier output, the summation circuit must divide by 2 the signal obtained after the 50 Ω series termination. The gain of the sum is given by :

$$\frac{V_{out}(s)}{I_{in}(s)} = \frac{1}{2}\frac{R_C}{R_i}(1-\alpha)(1-\beta) \tag{7}$$

where i = 1 to 16, α and β represent the loss of signal due respectively to the White follower and the finite input impedance. R_C and R_i are chosen to compensate these losses. The need of speed sets the choice of the transistors. For the White follower, the BFR92A gives a 91 KΩ input impedance in parallel with R_C : then, the risetime is around 14 ns for 10% signal loss. Each channel of the sum sees in parallel with its input impedance a 65 Ω resistor to ground due to the 15 other inputs. A significant part of signal can be lost in this resistor if the input impedance of the circuit is not small enough. Therefore, this impedance $Z_{in} = 26/I_E + R_B/\beta$, must be as low as possible ; R_B is taken at the minimum value to avoid oscillations, I_E is determined by R_E at a maximum value

to avoid saturation on the collector of the first transistor and $\beta = 30$ is given by the choice of a fast input pnp transistor (BFT92), which gives $Z_{in} = 8.4\ \Omega$. The loss of signal due to this input impedance is around 12%. The signals at the output of the transceiver with and without summation are compared in fig. 8.

This circuit has been improved for speed but at the expense of noise (Cf. section 4.2).

3.4 Transceiver board

Using surface mounted components, 32 channels plus 2 summation circuits have been laid out on a 105 mm wide by 210 mm long card. The width of the card is fixed by the output connectors which must accommodate 32 differential signals and their ground : it is done by two 3 row connectors where the first row is for the positive output, the second row for the negative output and the last one for the ground. On the opposite side, the 32 signals come into the card through also a 3 row connector but the ground is in the central row as the signals arrive by coaxial cables ; the width of this side is limited by the diameter of the feedthrough. A photograph of this board is shown in fig. 9.

On the board, the power supplies and ground are provided by layers. Moreover, the input and output tracks are controlled impedance lines ; which leads to a 6 layers board.

The 2 summation circuits are located near the input connector.

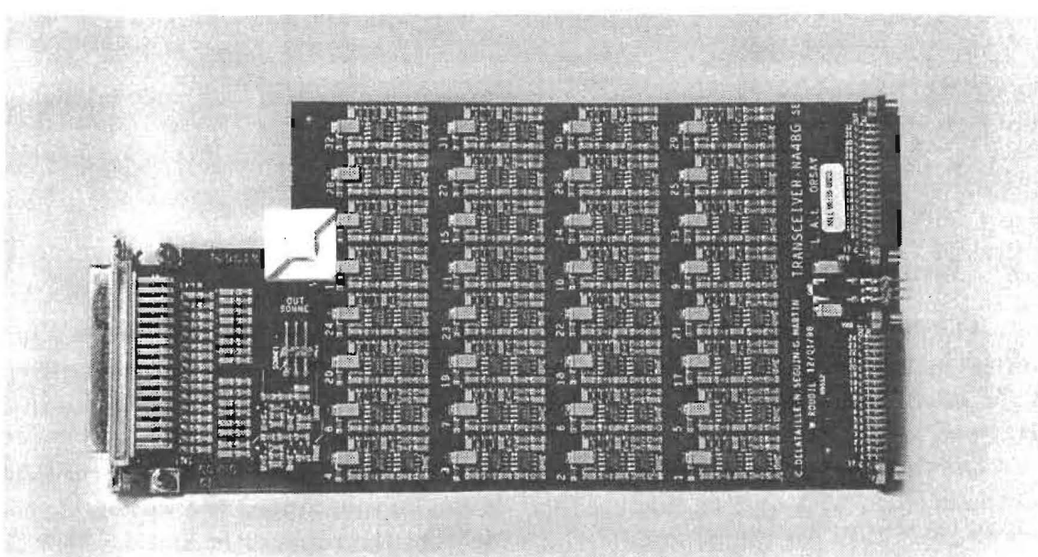

Figure 9: Photography of a transceiver card

4 Measurement results

4.1 Output signal

Fig. 10(a) shows the differential signals at the transceiver output for 25 GeV (65 μA) at the preamplifier input. The signal is measured at the end of a 10 meter long cable to take into account the skin effect. The output rise time (10 - 90 %) is 24.4 ns and the amplitude is ±450 mV, which matches the gain requirements before cable.

The pole-zero effect is shown in fig. 10(b) where the output signal, before cable and with a fast rise time constant (10 ns), is compared to the input signal of the transceiver coming from the preamplifier with a rise time constant of 150 ns.

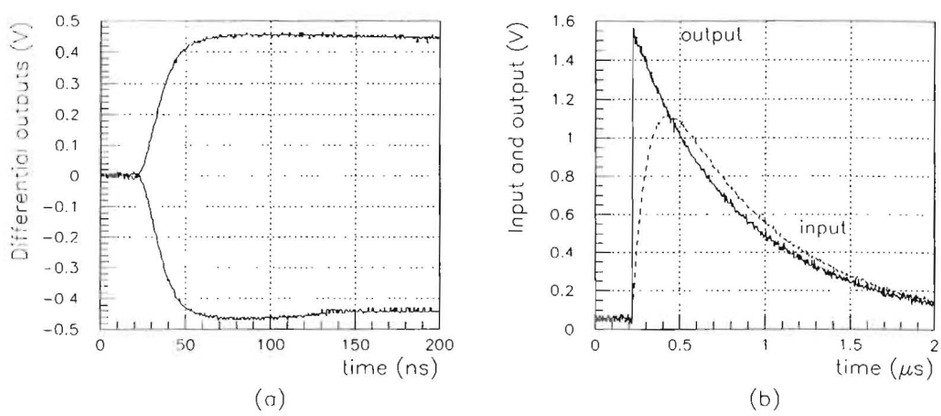

Figure 10: Differential signals at the transceiver output after 10m long cable (a) and positive output compared to the transceiver input (b)

4.2 Noise

The output noise spectral density of the transceiver alone was measured as a function of frequency. The division of this measure by the gain of the transceiver at the frequency of the maximum gives the input noise spectral density. This spectrum is shown in fig. 11(a) and gives a maximum value of 1.8 nV at 7 MHz.

On the H4 test beam at CERN [9], the total noise was 7 MeV for the complete electronic chain with a 75 ns shaping time. It can be split among the various elements as follows : 4.5 MeV for the preamplifier, 2.4 MeV for the transceiver and 4.5 MeV for the CPD. The fig. 11(b) shows the noise in MeV for the complete chain on the detector and for the transceiver alone, as a function of the peaking time at the shaper output.

The input noise density of the summation circuit followed by the transceiver presents a maximum value of 25 nV/$\sqrt{\text{Hz}}$ at 7 MHz. This value, similar than four times the preamp output (the circuit sums 16 preamplifiers), multiplies by $\sqrt{2}$ the total noise : this is due to the optimisation of speed for the summation circuit at the expense of the noise performance (Cf. section 3.3).

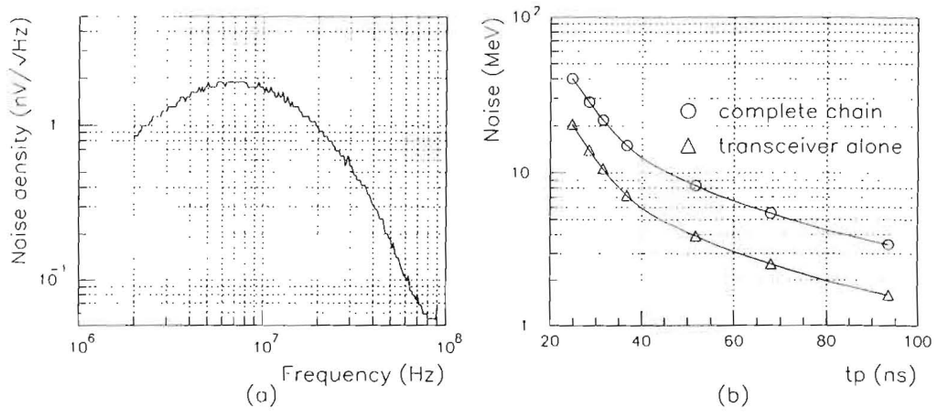

Figure 11: Input noise spectral density of the transceiver as a function of frequency (a) and noise on the detector as a function of the signal peaking time for the complete chain and the transceiver alone (b)

4.3 Linearity

The linearity is measured for a chain including an injection system, a preamplifier, a transceiver and a CRRC2 shaping at 50 ns. The integral non-linearity[14] is around 0.1 % for a maximum output signal of ± 1.5 V (75 GeV at the input).

The detector signal decays linearly in around 3 μs (triangular shape) : so, the differential linearity[15] must be good enough to allow a precise measurement of a photon which piles up on an accidental. This non-linearity presents a very little slope which is not critical.

The integral and differential non-linearity of the transceiver as a function of the input signal in GeV are shown in fig.12.

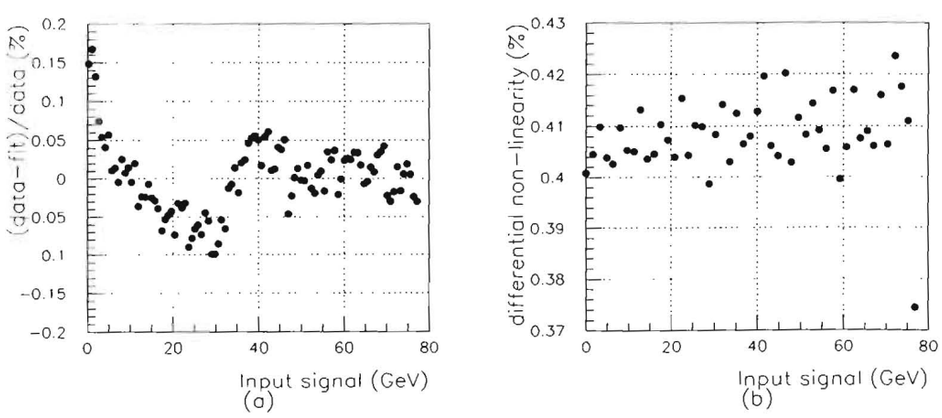

Figure 12: Integral (a) and differential (b) non-linearity of the transceiver

[14]The integral non-linearity is the residuals to best line fit divided by the maximum amplitude.
[15]The differential linearity is the linearity of the derivative.

4.4 Uniformity

Uniformity between cards but also within one board is an important issue to obtain high precision measurements. A small amplitude variation is achieved by good precision on the discrete components (1 % for resistors and 2 % for capacitors). The propagation time uniformity is obtained by using same length cable for all cards and careful routing of the signals on the card. The peaking time was measured at the output of a chain including a preamplifier, a transceiver and a CRRC2 shaper at 50 ns with and without a 10 meter long cable between transceiver and shaper. The scattering of this peaking time is drawn in fig. 13 as a function of the transceiver channel number. These curves show that the time dispersion measurement is more important in the cable (± 0.5 %) than in the board (± 0.2 %) : the channels 1 to 8 and 17 to 24 are in the same cable.

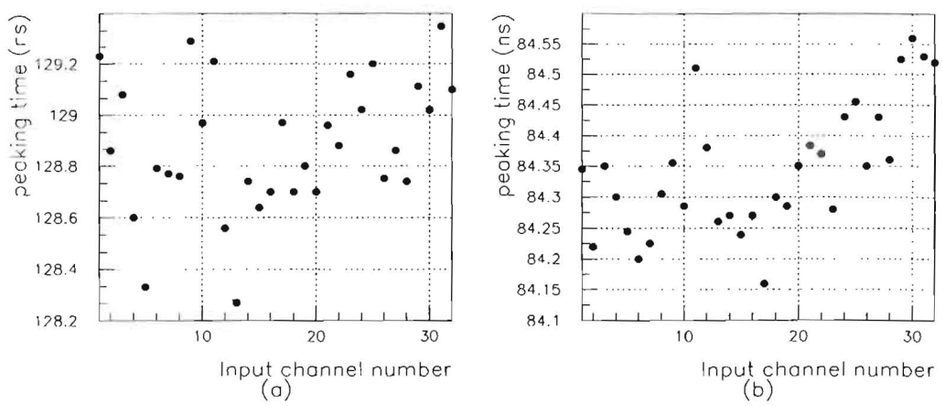

Figure 13: Scattering of the peaking time, with (a) and without (b) 10 meter long cable, as a function of the transceiver channel number.

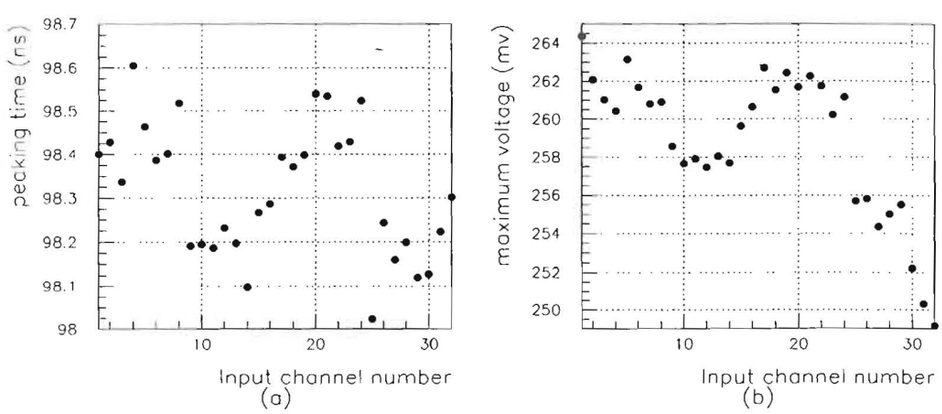

Figure 14: Scattering of the peaking time (a) and the amplitude (b) of the summation circuit as a function of the input channel number.

For the summation circuit, the fig. 14 shows the scattering of the peaking time and the amplitude for a chain including a preamplifier, the summator, the transceiver and a

CRRC2 shaper at 50 ns. This dispersion inside one sum is very low but the non-uniformity between various sums is more important because it depends on the behaviour of the input transistor. Channels 1 to 8 and 17 to 24 are summed together in a first sum and the other channels are summed in another one : the variation of the peaking time is 0.07 % for the two sums and the variation of the maximum is 0.4 % for the first sum and 1.2 % for the second sum.

4.5 Output common mode and power supply rejection ratios

The output common mode rejection ratio (CMRR) is measured by putting a source on an output and looking the result on the other output. The CMRR, presented in fig.15 for the two outputs, is obtained by simulation : it is better than 50 dB all over the frequency range.

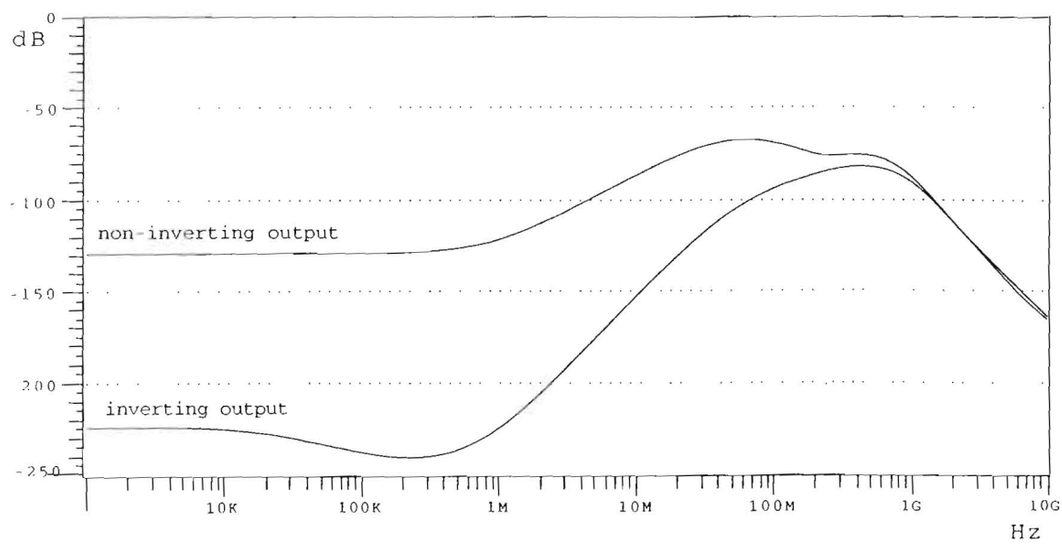

Figure 15: Output common mode rejection ratio.

The power supply rejection ratio is similar for the positive and negative supplies. It is larger than 50 dB at low frequency and goes up to 20 dB at 10 MHz.

4.6 Power dissipation and cost

To insure a good linearity over the whole dynamic range, the power supplies of the operational amplifiers are set at ± 6 V. This gives a dissipation of 310 mW per channel. The dissipation of the complete card is around 10 Watts (310 mW for each of the 32 channels plus the two summation circuits).

One channel costs around 12 CHF including board, components and connectors but not the power supplies and the cables going to the CPD.

5 Conclusion

A low noise circuit has been designed which fulfils the NA48 requirements and has been used for data taking since August 1996.

References

[1] P.Calafiura and A.Ceccuci, The performance of Liquid Krypton calorimeter and the neutral reconstruction, NA48-note 1995-4.

[2] C. Cerri, The NA48 liquid krypton calorimeter : electrode structure, front-end electronics and calibration - 6th international conference on calorimetry in high energy physics, Frascati, June 8-14, 1996.

[3] R. L. Chase et al. "Experimental results on cable-coupled preamplifiers (ØT)" NIM A343 (1994) 598-605.

[4] V. Radeka et al. "Performance and reliability of Si cryogenic preamplifiers for noble liquid calorimetry", 5th international conference on calorimetry in high energy physics, Brookhaven National Laboratory, 26 sep-1 oct 1994.

[5] V. Radeka, S. Rescia "Speed and noise limits in liquid ionization calorimetry" NIM A325 (1988) 228-242

[6] C. de La Taille "Electronic noise in LAr calorimetry" CERN Internal Note : RD3 Note 45.

[7] C. de La Taille et al., A low noise transceiver for the NA48 liquid krypton calorimeter - 6th international conference on calorimetry in high energy physics, Frascati, June 8-14, 1996.

[8] F. Bal et al., Performances of the CPD prototype module, NA48-note 1996-1.

[9] J.C. Chollet et al., Analysis of 1995 H4 data, NA48-note 1995-30.